Materials Horizons

# Super-Soft Solvent-Free Bottlebrush Elastomers for Touch Sensing



| | |
|---|---|
| Journal: | *Materials Horizons* |
| Manuscript ID | MH-COM-06-2019-000951.R1 |
| Article Type: | Communication |
| Date Submitted by the Author: | 01-Aug-2019 |
| Complete List of Authors: | Reynolds, Veronica; University of California Santa Barbara, Materials<br>Mukherjee, Sanjoy; University of California Santa Barbara,<br>Xie, Renxuan; University of California Santa Barbara, Materials<br>Levi, Adam; University of California Santa Barbara, Chemistry and Biochemistry<br>Atassi, Amalie; University of Florida, Materials Science and Engineering<br>Uchiyama, Takumi; Tokyo Institute of Technology, Materials Science and Engineering<br>Wang, Hengbin; University of California Santa Barbara, Mitsubishi Chemical Center for Advanced Materials<br>Chabinyc, Michael; University of California Santa Barbara<br>Bates, Christopher; University of California Santa Barbara, Materials |
| | |

## NEW CONCEPT STATEMENT

In this manuscript, we demonstrate a method to enhance the sensitivity of capacitive pressure sensors, which function by the reversible deformation of an elastomeric dielectric layer. Previous developments in this arena have focused on foaming or micropatterning techniques to reduce the effective elastomer modulus and increase sensitivity, but these approaches increase process complexity and cost. Here, we present an alternative strategy rooted in molecular design that leverages the inherently soft characteristic of bottlebrush polymers. Capacitive pressure sensors constructed with bottlebrush dielectric elastomers are optically transparent, flexible, and provide a significant performance improvement beyond traditional designs while preserving device robustness and manufacturing simplicity.

# Super-Soft Solvent-Free Bottlebrush Elastomers for Touch Sensing

Veronica G. Reynolds[†∇^], Sanjoy Mukherjee[‡∇^], Renxuan Xie[†∇], Adam E. Levi[+∇], Amalie Atassi[‖], Takumi Uchiyama[⊥], Hengbin Wang[∇], Michael L. Chabinyc[†∇*], Christopher M. Bates[†+§∇*]

[†]*Materials Department,* [‡]*Materials Research Laboratory,* [+]*Department of Chemistry and Biochemistry,* [§]*Department of Chemical Engineering, and* [∇]*Mitsubishi Chemical Center for Advanced Materials, University of California, Santa Barbara, California 93106, United States*

[‖]*Department of Materials Science and Engineering, University of Florida, Gainesville, Florida, United States*

[⊥]*Department of Materials Science and Engineering, Tokyo Institute of Technology, Tokyo, Japan*

[^]*These authors contributed equally*

**Keywords:** bottlebrush polymer, pressure sensor, elastomer, sensor skin

## TABLE OF CONTENTS

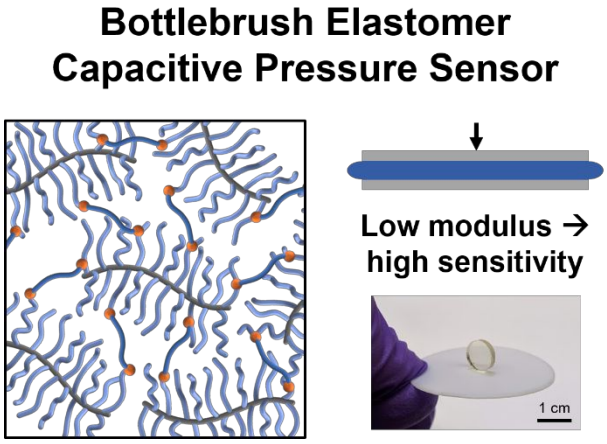


High sensitivity capacitive pressure sensors can be created with bottlebrush dielectric layers that overcome the limitations of traditional polymeric materials.

**ABSTRACT**

The sensitivity of capacitive pressure sensors is primarily determined by the modulus of a soft dielectric layer that reversibly deforms to produce an electrical signal. Unfortunately, the mechanical properties of conventional linear networks are constrained such that a lower limit on softness translates to poor capacitive pressure sensor performance. Here, we overcome this paradigm by leveraging the intrinsic "super-soft" characteristic of bottlebrush polymers. A simple light-induced crosslinking strategy is introduced to facilitate device fabrication and parallel plate capacitive pressure sensors constructed with these bottlebrush polymer networks exhibit up to a 53× increase in sensitivity compared to traditional material formulations, e.g., Sylgard 184. This combination of contemporary synthetic chemistry and application-driven materials design accentuates the opportunities available at the intersection of science and engineering.

## INTRODUCTION

Sensor skins are large area electronic devices that translate input stimuli into electrical signals for robotics and wearable electronics.[1,2] Pressure is a critical input in these applications because it provides environmental awareness that can be used to tune interaction with the surroundings. Key regimes include 1–10 kPa (touch sensing; intraocular and intracranial pressures) and 10–100 kPa (pulse monitoring).[3] Pressure sensors can be formed using a variety of materials, but dielectric polymers provide unique advantages versus inorganic options, such as high elongation at break and ease of processing for large area devices.

Capacitive pressure sensors (CPSs) are devices that report a capacitance change upon deformation of a dielectric layer.[3] The most basic CPS architecture is a parallel plate capacitor that can be readily formed with soft materials. Elastomer-based CPSs comprise an elastic dielectric layer sandwiched between two electrodes. In these devices, the sensitivity ($S$) is governed by the elastomer modulus (Figure 1) — softer materials produce higher sensitivity because an applied pressure causes a larger change in thickness (and thus a bigger change in the capacitance). However, CPSs have traditionally suffered from low sensitivity; often, more complex devices are needed to amplify signals in the low pressure regime, for example where a dielectric layer is also the gate of a transistor.[3,4] While traditional polymers do not satisfy current demands for soft dielectric elastomers, recent synthetic advances in macromolecular design present opportunities to control macroscopic properties with unprecedented tunability.

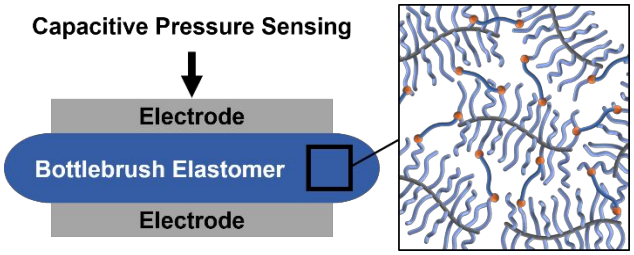


**Figure 1.** Illustration of a parallel plate capacitive pressure sensor fabricated with a bottlebrush polymer dielectric elastomer. Since sensor response scales inversely with elastomer modulus, "super-soft" bottlebrush networks improve sensitivity relative to traditional linear analogues. In the network illustration on the right, orange spheres represent productive crosslinking points that connect individual bottlebrush molecules.

Conventional elastomeric dielectric layers are usually formed from crosslinked networks of linear polymeric precursors. For example, poly(dimethylsiloxane) (PDMS) is commonly used in soft robotics and sensor skins because it is commercially available in various formulations such as Sylgard 184 (Dow Corning) and Ecoflex (Smooth-On Inc.).[5] Additional benefits of PDMS include its modest dielectric constant circa 2.3–2.8, high electrical resistivity, and nontoxicity.[6] In the field of dielectric elastomers, the VHB series of polyacrylate foam adhesives (3M) is also widely used for dielectric actuation.[7] Unfortunately, these and other linear elastomer networks exhibit a well-known lower bound on stiffness (circa $10^3$ kPa) that is characteristic of entangled polymers, thus placing an upper limit on the sensitivity of CPSs formulated therefrom.[2]

Numerous strategies have been devised to achieve higher sensitivity CPSs with conventional elastomers. One way to reduce the modulus of an elastomer involves partial crosslinking, effectively rendering the uncrosslinked polymer chains diluents and turning the resulting material into a gel (swollen network). The use of partially crosslinked or solvent-swollen networks can improve the conformability and sensitivity of CPSs,[8,9] but risks leachability and sacrifices rheological stability. An alternative to using gels is reducing the effective modulus of

the dielectric layer by incorporating air. Sylgard 184 can be micropatterned using a multistep molding process to create linear and pyramidal features on the micron scale.[4] These air–elastomer composites reduce the effective modulus of the dielectric layer by removing material, therefore amplifying pressure and providing space for the elastomer to deform. Elastomer foams — a different type of air–elastomer composite — have similar mechanical properties but are made through different processing routes. For example, porous elastomer layers can be formed by incorporating sacrificial particles, commonly sugar or salt granules, that are dissolved after curing the network (referred to as solid particle leaching).[10–13] Another technique involves the dispersion of water droplets into the elastomer matrix and subsequent evaporative removal post-curing.[14] While these routes have been shown to reduce effective modulus and improve CPS sensitivity, they require complex fabrication techniques and result in devices that are susceptible to contaminant ingress and response drift due to humidity.

Here, we introduce a new approach to create high sensitivity CPSs by designing dielectric elastomers based on bottlebrush polymers. This highly branched architecture tends to minimize chain entanglements, resulting in "super-soft" materials with a significantly lower bulk shear modulus than linear analogues (circa 1–100 kPa).[15,16] Figure 2 illustrates the two key ingredients in our formulations: (1) well-defined bottlebrush precursors comprising a long backbone and densely-grafted side-chains with chemical degrees of polymerization denoted as $N_{BB}$ and $N_{SC}$, respectively,[17–19] and (2) a photo-crosslinkable bis-benzophenone additive that includes a customized linker to promote miscibility with the bottlebrushes at room temperature for facile mixing without solvent. We demonstrate that using PDMS-based bottlebrush elastomers as dielectric layers in CPSs increases sensitivity by 3–53× compared to conventional elastomers.

These improvements are comparable to, or better than, previous microstructuring strategies, yet involve significantly simpler processing steps.

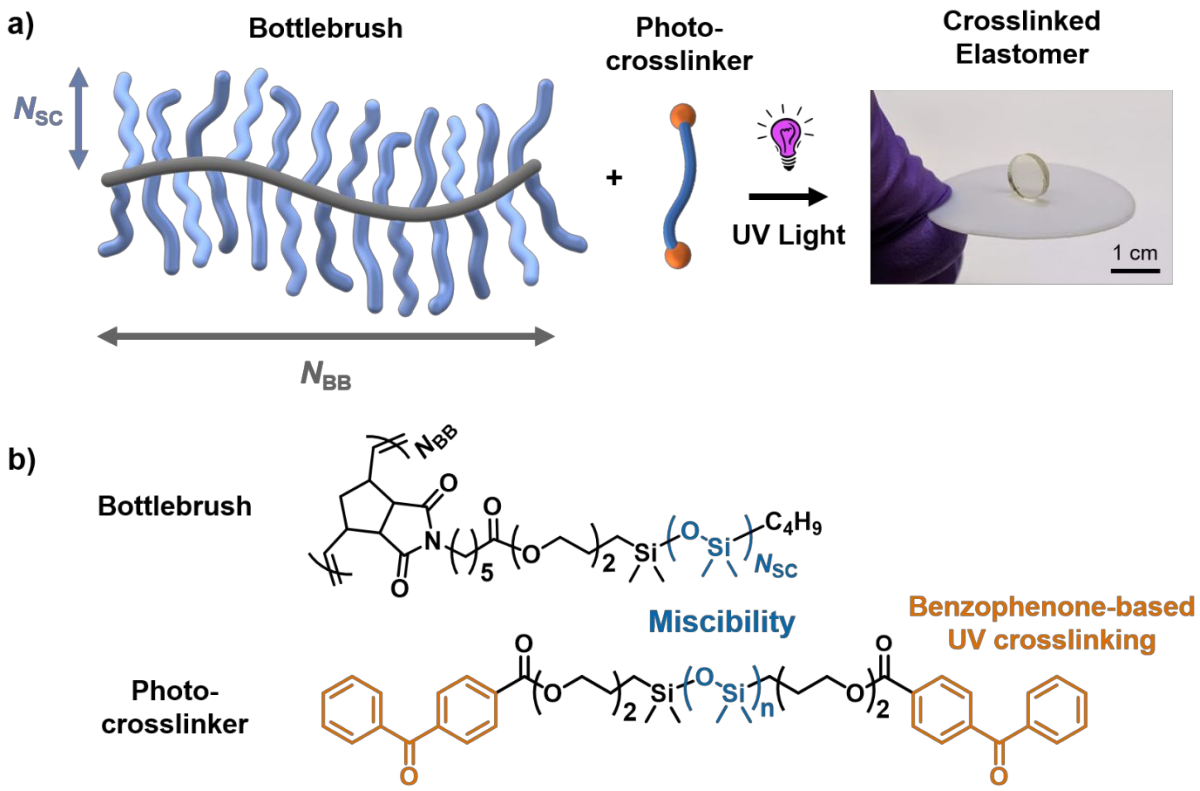


**Figure 2.** Photo-crosslinkable bottlebrush dielectric elastomer formulations. **a)** Key ingredients include well-defined bottlebrush molecules with backbone and side-chain degrees of polymerization $N_{BB}$ and $N_{SC}$, respectively, and a bis-benzophenone-based photo-crosslinker. All components are miscible at room temperature to produce a viscous liquid mixture. Subsequent crosslinking with UV light creates an elastomeric solid. **b)** Chemistry of the PDMS bottlebrush polymer and PDMS-based bis-benzophenone photo-crosslinker. Full synthetic details are available in the Supplementary Information.

## Results and Discussion

### *Molecular Design and Synthesis*

Our initial design for solvent-free bottlebrush dielectric elastomers is based on PDMS due to its favorable rheological properties, optical transparency, non-toxic nature, and relatively high entanglement molecular weight ($M_e$ = 21–33 kDa).[6] A PDMS macromonomer ($M_n$ = 5.3 kg mol$^{-}$

$^{1}$, $Đ$ = 1.1, $N_{SC}$ = 68) was synthesized from commercially-available poly(dimethylsiloxane) by installing a norbornene group on one end (see Supplementary Information for details). Subsequent grafting-through ring-opening metathesis polymerization (ROMP) catalyzed by a Grubbs 3rd generation catalyst produced a library of bottlebrush polymers with constant PDMS side-chain degree of polymerization ($N_{SC}$ = 68) and variable poly(norbornene) backbone lengths ($N_{BB}$). An advantage of this synthetic approach is the ability to fully characterize well-defined bottlebrush precursors[20,21] (see Table S1 for a summary) before subsequent crosslinking reactions, in contrast to *in situ* polymerization methods that simultaneously construct the bottlebrush architecture and crosslink chains.[22]

The PDMS bottlebrush polymers are viscous liquids (zero-shear viscosity $\eta_0$ = 2–55 Pa·s) that require crosslinking to form a solid elastomer network. Network formation was achieved by designing a PDMS-based benzophenone (BP) photo-crosslinker, which we envisioned would simplify the synthesis of solvent-free elastomers and facilitate integration of bottlebrush materials into useful devices. The BP unit has a relatively weak absorption band near 350 nm (n→π*) and strong absorption bands near 200–250 nm (π→π*). When irradiated with a 350 nm light source, triplet excited states of benzophenone abstract hydrogen atoms from nearby alkyl moieties via radical pathways. The resulting reactive species can undergo C–C coupling reactions; through this mechanism, a molecule with two BP moieties can covalently crosslink distinct polymer chains. To obtain a photo-crosslinker that homogeneously mixes with PDMS bottlebrushes without any additional solvent, we functionalized di-hydroxy telechelic PDMS ($M_n$ = 6.0 kg mol$^{-1}$, $Đ$ = 1.3, $N$ = 72) with BP moieties at both termini. This design is critical since small molecule bis-benzophenones lacking a bridging PDMS chain were immiscible with PDMS-based

bottlebrush polymers, even at elevated temperatures. Our solvent-free mixing strategy provides a facile route to an all-solids, super-soft dielectric layer.

***Rheology of Benzophenone-Crosslinked PDMS Bottlebrush Elastomers***

Various formulations of PDMS bottlebrush polymer and PDMS crosslinker were prepared to investigate the effects of molecular design on network properties and CPS performance. Samples are referred to as $\mathrm{PDMS}_{68}^{N_{BB}}$-*XX*, where $N_{BB}$ is variable, $N_{SC} = 68$ is held constant, and *XX* is the number of crosslinkers per bottlebrush molecule. The range of architectures and formulations explored produced bottlebrush elastomers with moduli spanning nearly two decades.

Rheological analysis with *in situ* light exposure (365 nm, 150 mW/cm$^2$) indicates the PDMS bottlebrush formulations described above are UV-crosslinkable at room temperature with a relatively fast gel time ($G' = G''$) circa 100 sec for thick layers (≈0.4 mm) (Figure 3a). Continued illumination further increases the shear modulus over the course of about 1000 sec, resulting in a plateau value that depends on crosslinker loading. As expected, higher crosslinker concentration increases both curing time and the final modulus. Frequency sweeps (Figure 3b) of fully cured samples at room temperature further indicate the plateau storage modulus (defined at 0.001 rad/s by Fast Fourier Transformed (FFT) stress relaxation or creep results) depends on $N_{BB}$. The softest formulations occur at large $N_{BB}$, which produces longer network strands on average, in agreement with previous work.[23] Importantly, all of these materials are considerably softer — by 1–2 orders of magnitude — than linear PDMS that was thermally cured at 150 °C for 30 min (c.f., Sylgard 184 in Figure 3b). Moreover, for three different backbone lengths ($N_{BB}$ = 20, 99, and 235), low crosslinker loadings still produce excellent gel fractions (>85%) as measured via mass loss after solvent soaking (24 hr in toluene). The gel fraction correlates with curing completeness (percentage of polymer chains incorporated into the elastic network) and is critical for elasticity,

non-leachability, and device stability. This combination of soft mechanical properties ($G'$ = $10^4$–$10^5$ Pa) and high gel fraction highlights the advantages of the bottlebrush architecture in comparison to linear alternatives.

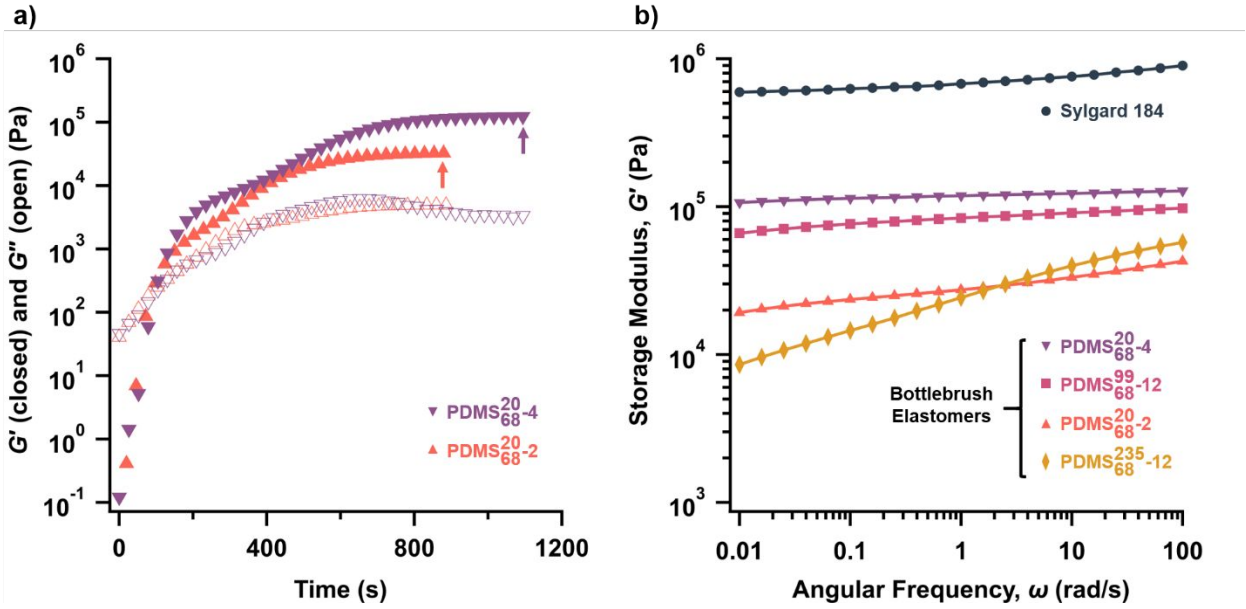


**Figure 3. a)** PDMS bottlebrush formulations are photo-crosslinkable as evidenced by rheological analysis of PDMS$_{68}^{20}$-2 and PDMS$_{68}^{20}$-4 under UV light exposure (365 nm, 150 mW/cm$^2$; exposure begins at $t$ = 0). **b)** Frequency sweeps indicate the plateau storage modulus can be tuned by $N_{BB}$ and crosslinker loading. Measurements were taken at 21 °C and 1% strain. Loss moduli and FFT results are available in the Supplementary Information.

### *Capacitive Pressure Sensor Fabrication and Performance*

Capacitive pressure sensors were fabricated by laminating molded elastomer discs to flexible and transparent indium-tin-oxide-(ITO)-coated poly(ethylene terephthalate) (PET) electrodes mounted on glass substrates (Figure 4). The choice of electrode enabled visual inspection of the elastomer–electrode interface (the quality of which is critical to device performance) and additionally resulted in transparent and flexible (Figure S17) sensors. The dielectric constant of the PDMS bottlebrush networks is 2.6 at frequencies of 100 to $10^5$ Hz, a

value identical to Sylgard 184 (Figure S11). Based on parallel plate capacitance and rubber elasticity models, CPS sensitivity (defined as the slope of the sensor response curve, $S = \mathrm{d}(\Delta C/C_0)/\mathrm{d}\sigma$) should scale inversely with the modulus of the elastomer (see Supplementary Information). The pressure sensors were tested by simultaneously measuring capacitance with an LCR (inductance, capacitance, resistance) meter and applied force. Sensor response curves were collected in the 0–50 kPa range with an S-beam load cell in a displacement-controlled compression tester. Pressure cycling curves of the sensors were collected using a TA Instruments Dynamic Mechanical Analyzer (DMA) 850 to apply a sinusoidal force program at specific frequencies. Note that for the cycling data, the relative change in capacitance was calculated relative to a pre-loaded (rather than unloaded) state. Care was taken to eliminate stray capacitive effects so that the sensor response was dominated by the mechanics of the elastomer layer. The sensors would ideally be fully shielded from stray capacitance of the leads, but the requirements of our mechanics-focused design — complete transfer of applied pressure to the elastomer disc and freedom for lateral expansion of the elastomer — limited such a setup. The test environment was grounded and kept constant for each elastomer tested.

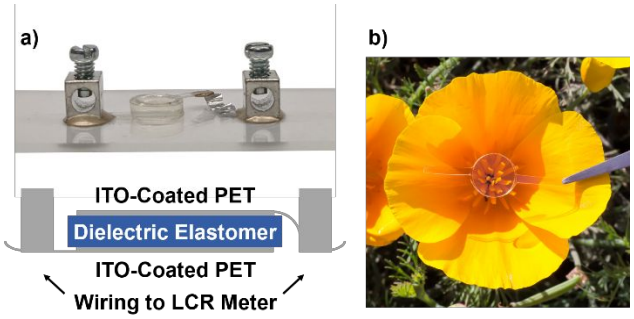


**Figure 4. a)** Optical photograph and accompanying schematic of the capacitive pressure sensor devices studied herein. ITO-coated PET electrodes enabled a visual check of interfaces and screw terminals attached with conductive epoxy ensured repeatable connection to the LCR meter. **b)** The sensor has excellent optical

properties with <1% haze over the majority of the visible spectrum (transmittance and haze spectra are available in the Supplementary Information, Figure S12).

The modulus of the bottlebrush elastomers is controllable by crosslinker concentration and can improve the sensitivity of CPSs. Figure 5a shows the sensor response curves for four PDMS bottlebrush networks ($PDMS_{68}^{20}$-2, $PDMS_{68}^{20}$-4, $PDMS_{68}^{99}$-12, $PDMS_{68}^{235}$-12) and a reference linear elastomer (Sylgard 184). The response of the Sylgard 184 sensor quickly saturates relative to the bottlebrush elastomer sensors. For the bottlebrush networks, moving from 4 to 2 crosslinkers per chain produces a significant increase in sensitivity concomitant with a reduced $G_0$. The sensor made with the softest polymer, $PDMS_{68}^{235}$-12 ($G_0$ = 6.2 kPa) exhibits extremely high sensitivity. As compared with the Sylgard 184 sensor, it has 22× higher sensitivity in the low pressure (0–10 kPa) regime and 53× higher sensitivity in the high pressure (20–50 kPa) regime. Sensitivities for all sensors measured are summarized in Table 1; note that $S_{Y-Z}$ indicates the sensitivity in pressure regime *Y*–*Z* kPa. At the highest pressure of 50 kPa, strains occurring in the sensors ranged from 0.03 (Sylgard 184) to 0.38 ($PDMS_{68}^{235}$-12). All sensors tested exhibited response hysteresis at the strain rate used, meaning the unloading curve appears different than the loading curve. Hysteresis is common for sensors with dielectric elastomers and is most evident here for the lowest modulus elastomers with the largest magnitude signals. The capacitance of the two lowest modulus bottlebrush elastomer sensors did not return to the baseline at the end of the high pressure (0–50 kPa) response test, indicating either an undesirably slow relaxation response or permanent sample damage. The former seems more likely based on the low-frequency rheology data (Figure 3b) and visual evidence that suggests sample integrity. Further investigation into cycling stability using the DMA revealed a trade-off between sensitivity and baseline stability in pressure regimes that approach significant strains. Figure 5b shows that in the medium pressure regime (1–21 kPa), the

sensor prepared with $PDMS_{68}^{235}$-12 undergoes some baseline drift over time while one prepared with $PDMS_{68}^{99}$-12 remains relatively stable. These data suggest that high sensitivity and baseline stability may be achieved by appropriately matching a bottlebrush elastomer with the pressure range of interest.

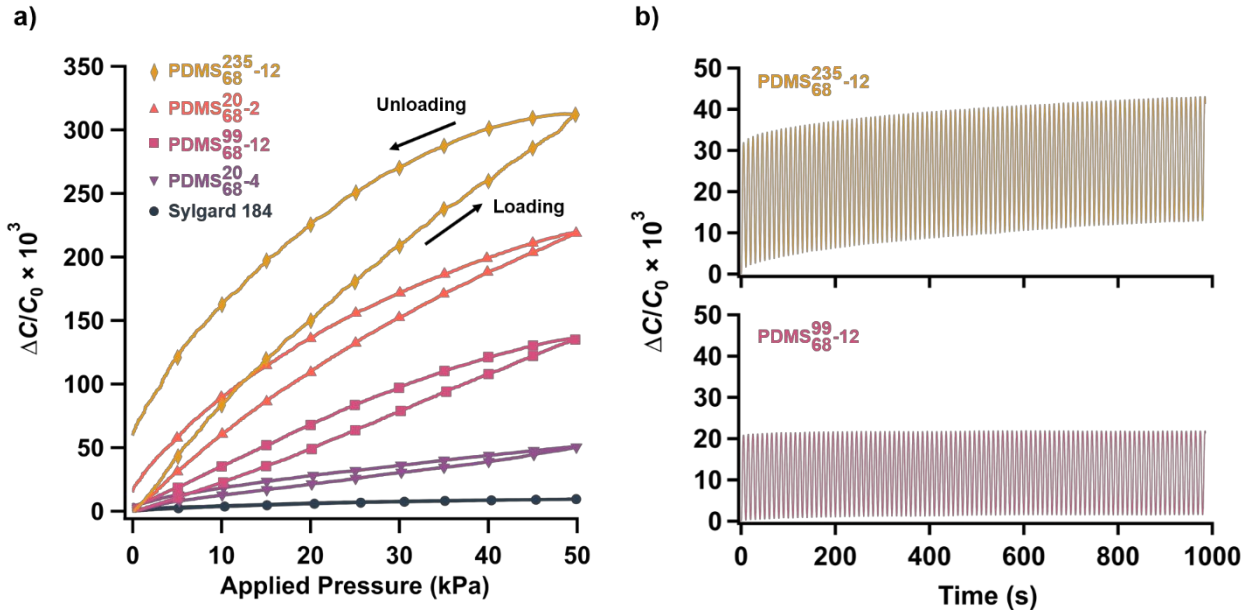


**Figure 5. (a)** Sensor response curves (relative change in capacitance vs. applied pressure) show the bottlebrush elastomers enable improved sensitivity compared to crosslinked linear PDMS (Sylgard 184). Sensors were loaded and unloaded at a strain rate of 0.001 $s^{-1}$. **(b)** Cycling tests show a trade-off between sensitivity and baseline stability. The sensors were cycled at 0.1 Hz with an 11 kPa pre-load and a 10 kPa wave amplitude, resulting in oscillation between 1–21 kPa. Note that the amplitude of oscillation remains relatively constant even as the baseline drifts.

**Table 1.** Measured sensitivities for the bottlebrush elastomer and Sylgard 184 sensors.

| Sample ID | $G_0$ (kPa) | $S_{0-10}$ ($kPa^{-1}$) | $S_{0-10}/S_{Sylgard}$ | $S_{20-50}$ ($kPa^{-1}$) | $S_{20-50}/S_{Sylgard}$ |
|---|---|---|---|---|---|
| Sylgard 184 | 520 | 0.0004 | - | 0.0001 | - |
| $PDMS_{68}^{20}$-4 | 92 | 0.0013 | 3.3 | 0.0009 | 9.0 |
| $PDMS_{68}^{99}$-12 | 53 | 0.0023 | 5.8 | 0.0029 | 29 |

| | | | | | |
|---|---|---|---|---|---|
| $PDMS_{68}^{20}$-2 | 16 | 0.0062 | 16 | 0.0036 | 36 |
| $PDMS_{68}^{235}$-12 | 6.2 | 0.0087 | 22 | 0.0053 | 53 |

The bottlebrush elastomer sensors exhibit high sensitivity at pressures under 1 kPa and additionally show rapid response times to pressure oscillations at 0.1 Hz (Figure 6). In considering higher frequency pressure application, the frequency-dependent modulus curves from our rheological studies can be used to identify appropriate limits. The two stiffer bottlebrush elastomers exhibit less frequency-dependent shear moduli between 0.01 and 100 rad/s, which is correlated with smaller hysteresis in the sensor response. The two softer bottlebrush elastomers exhibit some relaxation into the low frequency regime (i.e., < 0.1 rad/s), possibly resulting in the pronounced hysteresis for the sensor response at the strain rate of 0.001 $s^{-1}$. Further studies investigating the effect of bottlebrush architecture on frequency response may elucidate the cause of this slow relaxation and help minimize hysteresis through informed molecular design.

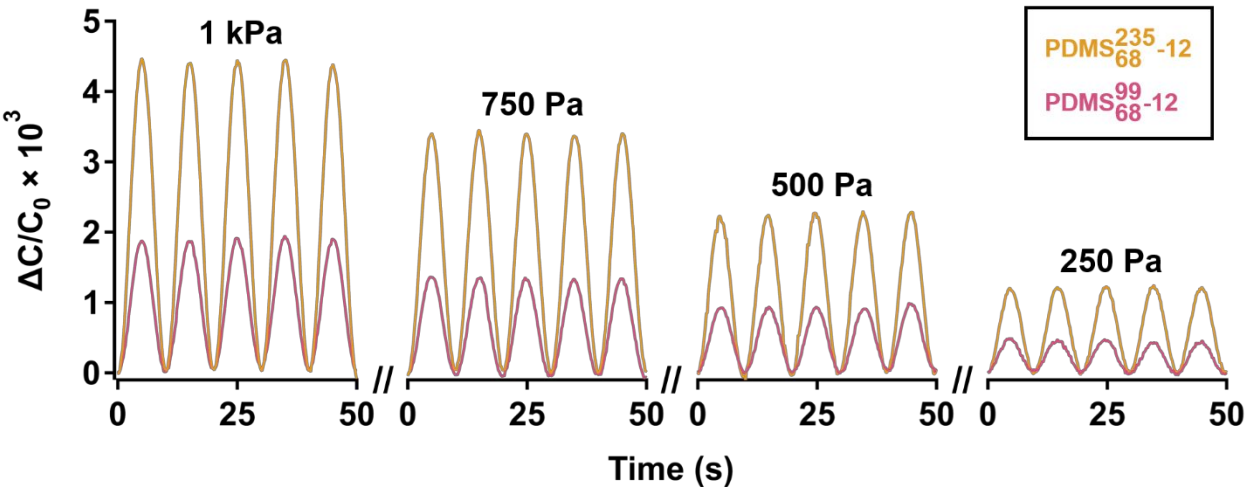


**Figure 6.** Low pressure cycling of the bottlebrush elastomer sensors shows high sensitivity in the 250 Pa – 1 kPa regime. The data shown were collected at a frequency of 0.1 Hz with the amplitude of pressure oscillation labeled above each dataset.

***Modeling the Modulus–Sensitivity Relationship***

The expected response of CPSs prepared with a uniform elastomer layer is more easily modeled than micropatterned or foamed alternatives. The compression of a dielectric elastomer layer between stretchable electrodes, assuming constant relative permittivity and incompressibility (Poisson's ratio, $\nu = 0.5$), will result in the relationship between relative change in capacitance $\Delta C/C_0$ and extension ratio in the direction of applied pressure $\lambda$ shown in Eq. 1:

$$\frac{\Delta C}{C_0} = \lambda^{-2} - 1 \tag{1}$$

The ITO-coated PET film electrodes used in this work are undersized and inextensible relative to the soft and elastic dielectric. Applying a constant area assumption to the derivation with stretchable electrodes gives the new relationship shown in Eq. 2:

$$\frac{\Delta C}{C_0} = \lambda^{-1} - 1 \tag{2}$$

Following this constant area relationship, the pressure sensor sensitivity $S$ can be related to the shear modulus, $G$, using the network theory of rubber elasticity,[24] as:

$$S = \frac{1}{G(\lambda + \lambda^{-1} + 1)} \Rightarrow \frac{1}{3G} \text{ (small strain limit)} \tag{3}$$

Derivations of the above expressions may be found in the Supplementary Information. We expect that practical sensors will deviate from the predicted behavior. In practice there are parasitic circuit elements in the detection circuit and the adhesion of the elastomer to the electrodes will limit free deformation of the polymer. The effect of parasitic circuit elements was found to be similar for all sensors (evaluated by comparing the measured capacitive signal to that expected by calculations using the measured strain). The adhesion of the elastomer to the electrodes inhibits lateral expansion, promoting bulging of the disc sidewall; the impact of this on stress–strain behavior has

been described through a geometric correction factor that increases the apparent modulus.[25,26] The effect of adhesion to the electrodes was found to become significant in the lower modulus elastomers, which deformed to higher strains in the pressure range tested. Further details can be found in the Supplementary Information. Despite the aforementioned non-idealities, the simple model (Eq. 3) was found to roughly capture the sensitivity–modulus scaling found in this work (Figure 7), with a good fit for low pressure (0–10 kPa) sensitivities of all sensors except for the lowest modulus bottlebrush elastomer, $PDMS_{68}^{235}$-12.

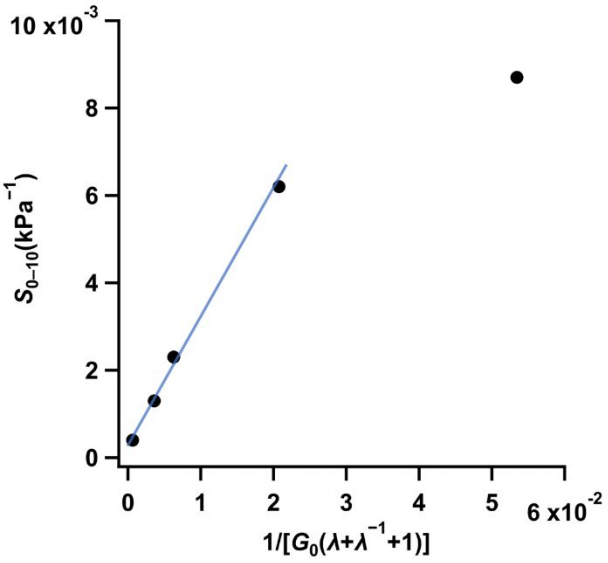


**Figure 7.** The simple model, which predicts a linear relationship between sensitivity and the modulus/extension ratio term, fits for all but the softest bottlebrush elastomer sensor.

The performance of CPSs is highly dependent on device design in addition to material selection and fair comparisons of sensitivity should therefore be made relative to a control sensor of the same design. Our work demonstrates sensitivity increases relative to a control ranging from 3.3× to 22× in the 0–10 kPa range and 9.0× to 53× in the 20–50 kPa range by using bottlebrush elastomers instead of traditional linear elastomers. In comparison, the micropatterning method for PDMS reportedly leads to a 28× sensitivity increase in the 0–2 kPa range and a 7.5× increase in

the 2–7 kPa range compared to an unstructured Sylgard 184 layer.[4] Introduction of microporosity reportedly results in an 8.2× sensitivity increase in the 0–10 kPa range and a 1.3× increase in the 10–100 kPa range (via processing with 10:1 sugar:Sylgard 184, 89.3% porosity).[12] In another study, a 38× sensitivity increase in the 0–5 kPa range was reported for a sensor with both a microporous dielectric layer and stretchable electrodes.[11] The performance of a broader range of sensors can be found in the Supplementary Information (Table S2). Notably, the air–elastomer composites exhibit declining sensitivities at high pressures — as air is displaced, the dielectric layer increasingly behaves like a bulk elastomer layer. The non-negligible gas permeability of PDMS adds complexity to this deformation behavior, i.e., it is not clear whether the gas simply leaks out of the sensor or permeates the PDMS.[6] Here, we achieve comparable, or better, performance through the use of a rationally designed all-solids material, rather than through complex processing. A combination of bottlebrush materials and porosity could conceivably result in even larger increases in sensitivity than achievable with either strategy alone.

## CONCLUSION

The use of super-soft bottlebrush elastomers as dielectric layers in solvent-free capacitive pressure sensors produces significant performance enhancements while preserving a simple and easily manufacturable design. Formulations that include a bis-benzophenone-based additive can be UV cured in minutes and the resulting mechanical properties are highly tunable via crosslinker loading and bottlebrush backbone degree of polymerization. Optimal designs reach moduli circa $10^4$–$10^5$ Pa, a factor of 10–100× smaller than conventional linear analogues. This greater deformability results in device sensitivities up to 53× higher than commercially available Sylgard 184, highlighting the potential of applying new polymeric materials in well-established device architectures.

**Experimental Methods**

PDMS bottlebrush elastomers were prepared by the addition of PDMS bis-benzophenone at molar concentrations varying between 2–12 crosslinkers per bottlebrush molecule. Rheology samples were cured *in situ* with the UV LED curing accessory for a TA Instruments AR-G2 rheometer (150 mW/cm$^2$, 365 nm). Pressure sensor samples were cured using a collimated LED (approximately 1 mW/cm$^2$, 365 nm; M365L2-C1, Thorlabs) or on the rheometer. These narrowband light sources avoid sample degradation issues that can occur with broadband UV sources (e.g., metal halide bulbs). Mixtures of bottlebrush polymer and photo-crosslinker were degassed in a vacuum oven at 100 °C for 3 hours before UV crosslinking to ensure the elimination of any air bubbles. The sensors were fabricated by crosslinking bottlebrush polymers in a poly(tetrafluoroethylene) mold (6.35 mm diameter by 1.55 mm thick disc) and laminating to ITO-coated PET electrodes (Thorlabs). The use of transparent electrodes enabled visual inspection of the electrode–polymer interface for bubbles and delamination. Electrical connection to the sensor was established by installing screw terminals (Keystone Electronics Corp.) with conductive epoxy (CW2400, Chemtronics).

For pressure sensor response curve measurements, a compression tester with a precision ball screw stage actuated by a micro-stepper motor was used to compress the sensors at a strain rate of 0.001 s$^{-1}$; a 5 N load cell was used to measure applied force, with its signal conditioned by a standalone strain gage amplifier. A laser extensometer (Electronic Instrument Research LE-01) was used to monitor sub-micron displacements for high resolution strain measurement. A glass spacer was used to electrically insulate the sensor from the compression tester and distribute the pressure across the sensor face; a rounded probe was used to ensure level compression. Pressure sensor cycling tests were collected with a TA Instruments DMA 850 using the parallel plate

compression clamp. A PTFE spacer was used to electrically insulate the sensor from the clamp. For both response curve and cycling tests, capacitance measurements were collected with a Keysight E4980A LCR meter, using a probing AC signal of 1 V / 100 kHz. To the greatest extent possible, the sensor test environment was grounded to the LCR meter to reduce electromagnetic interference effects.

## ASSOCIATED CONTENT

### Supplementary Information

Synthetic details, NMR, SEC-MALS, and rheology, data, sensitivity–modulus model derivation, comparison of experimental stress–strain curves to those predicted from rubber elasticity models.

## AUTHOR INFORMATION

### Corresponding Author

* cbates@ucsb.edu

* mchabinyc@engineering.ucsb.edu

### Author Contributions

Experiments were designed by V.G.R., S.M., R.X., M.L.C., and C.M.B. and performed by V.G.R., S.M., R.X., A.E.L., A.A., and T.U. The manuscript was written by V.G.R., S.M., R.X., M.L.C., and C.M.B. All authors have given approval to the final version of the manuscript.

### Notes

A provisional patent has been filed covering the results reported herein. The authors declare no other competing financial interest.

## ACKNOWLEDGMENT

Materials characterization was supported by NSF DMR 1436263. V.G.R. was partially supported by the National Science Foundation Graduate Research Fellowship Program. The research reported here made use of shared facilities of the UCSB MRSEC (NSF DMR 1720256), a member of the Materials Research Facilities Network (www.mrfn.org). Special thanks to Kirk Fields, Mechanical Test Lab, Department of Mechanical Engineering, UCSB and Prof. Yon Visell, Department of Electrical and Computer Engineering and Media Arts and Technology Program, UCSB for assistance with the pressure sensor test method development. Special thanks to the Helgeson Lab, UCSB for access to the AR-G2 rheometer and UV curing accessory.

## REFERENCES

1 J.-Y. Sun, C. Keplinger, G. M. Whitesides and Z. Suo, *Adv. Mater.*, 2014, **26**, 7608–7614.

2 S. Wagner and S. Bauer, *MRS Bull.*, 2012, **37**, 207–213.

3 Y. Zang, F. Zhang, C. A. Di and D. Zhu, *Mater. Horizons*, 2015, 2, 140–156.

4 S. C. B. Mannsfeld, B. C. K. Tee, R. M. Stoltenberg, C. V. H. H. Chen, S. Barman, B. V. O. Muir, A. N. Sokolov, C. Reese and Z. Bao, *Nat. Mater.*, 2010, **9**, 859–864.

5 F. Ilievski, A. D. Mazzeo, R. F. Shepherd, X. Chen and G. M. Whitesides, *Angew. Chemie - Int. Ed.*, 2011, **50**, 1890–1895.

6 J. E. Mark, *Polymer Data Handbook*, Oxford University Press, New York, 2nd edn., 2009.

7 P. Brochu and Q. Pei, *Macromol. Rapid Commun.*, 2010, **31**, 10–36.

8 K. F. Lei, K. F. Lee and M. Y. Lee, *Microelectron. Eng.*, 2012, **99**, 1–5.

9 Z. Lei, Q. Wang, S. Sun, W. Zhu and P. Wu, *Adv. Mater.*, 2017, **29**, 1700321.

10 O. Atalay, A. Atalay, J. Gafford and C. Walsh, *Adv. Mater. Technol.*, 2018, **3**, 1700237.

11 D. Kwon, T. I. Lee, J. Shim, S. Ryu, M. S. Kim, S. Kim, T. S. Kim and I. Park, *ACS Appl. Mater. Interfaces*, 2016, **8**, 16922–16931.

12 J. Il Yoon, K. S. Choi and S. P. Chang, *Microelectron. Eng.*, 2017, **179**, 60–66.

13 S. Kang, J. Lee, S. Lee, S. G. Kim, J. K. Kim, H. Algadi, S. Al-Sayari, D. E. Kim, D. E. Kim and T. Lee, *Adv. Electron. Mater.*, 2016, **2**, 1600356.

14 B. Y. Lee, J. Kim, H. Kim, C. Kim and S. D. Lee, *Sensors Actuators, A Phys.*, 2016, **240**, 103–109.

15 D. Neugebauer, Y. Zhang, T. Pakula, S. S. Sheiko and K. Matyjaszewski, *Macromolecules*, 2003, **36**, 6746–6755.

16 W. F. M. Daniel, J. Burdyńska, M. Vatankhah-Varnoosfaderani, K. Matyjaszewski, J. Paturej, M. Rubinstein, A. V. Dobrynin and S. S. Sheiko, *Nat. Mater.*, 2016, **15**, 183–189.

17 S. S. Sheiko, B. S. Sumerlin and K. Matyjaszewski, *Prog. Polym. Sci.*, 2008, 33, 759–785.

18 J. Rzayev, *ACS Macro Lett.*, 2012, 1, 1146–1149.

19 T. P. Lin, A. B. Chang, H. Y. Chen, A. L. Liberman-Martin, C. M. Bates, M. J. Voegtle, C. A. Bauer and R. H. Grubbs, *J. Am. Chem. Soc.*, 2017, **139**, 3896–3903.

20 Y. Xia, J. A. Kornfield and R. H. Grubbs, *Macromolecules*, 2009, **42**, 3761–3766.

21 S. Jha, S. Dutta and N. B. Bowden, *Macromolecules*, 2004, **37**, 4365–4374.

22 L. H. Cai, T. E. Kodger, R. E. Guerra, A. F. Pegoraro, M. Rubinstein and D. A. Weitz,

*Adv. Mater.*, 2015, **27**, 5132–5140.

23 M. Vatankhah-Varnosfaderani, W. F. M. Daniel, M. H. Everhart, A. A. Pandya, H. Liang, K. Matyjaszewski, A. V. Dobrynin and S. S. Sheiko, *Nature*, 2017, **549**, 497–501.

24 L. R. G. Treloar, *The Physics of Rubber Elasticity*, Oxford University Press, New York, 3rd edn., 1975.

25 A. N. Gent and P. B. Lindley, *Proc. Inst. Mech. Eng.*, 1959, **173**, 111–122.

26 A. N. Gent and E. A. Meinecke, *Polym. Eng. Sci.*, 1970, **10**, 48–53.